Original Article
pISSN 1738-2637
J Korean Soc Radiol 2012;66(6):551-558

대한영상의학회지

Three-Dimension Magnetic Resonance Lumbosacral Radiculography by Principles of the Selective Excitation Technique Imaging in the Diagnosis of Symptomatic Foraminal Stenosis

증후성 추공 협착증의 진단에서 Principles of the Selective Excitation Technique 영상기법을 이용한 삼차원 자기공명 요추천골 신경근조영술의 유용성

Ji Kyung Lim, MD, Woo Mok Byun, MD

Department of Radiology, College of Medicine, Yeungnam University, Daegu, Korea

Purpose: To investigate significance of three-dimension (3D) magnetic resonance (MR) lumbosacral radiculography by principles of the selective excitation technique (Proset) in the diagnosis of symptomatic foraminal stenosis.

Materials and Methods: A total of 288 foramina in 48 patients were analyzed (from L3-4 to L5-S1). Conventional spin echo sequence and 3D coronal fast-field echo sequences with selective water excitation by Proset were acquired. Through conventional MR imaging, the presence of lumbar foraminal stenosis was evaluated. Three morphologic changes (swelling, indentation, and tilting angle abnormality) of corresponding nerve roots were assessed on 3D MR lumbosacral radiculography. Relationships between the three morphologic findings and corresponding symptoms were evaluated.

Results: In 288 foramina, symptomatic and asymptomatic foraminal stenoses were found in 49 and 14 foramina, respectively. In symptomatic foraminal stenosis, swelling, indentation and tilting angle abnormality of the nerve root were found in 36, 18, and 10 foramina, respectively. One or more of the three findings was found in 46 foramina. In 12 foramina with asymptomatic foraminal stenosis, no morphologic changes were found. A statistically significant difference among three morphologic changes of nerve root in symptomatic foraminal stenosis was found (χ^2 test, $p < 0.001$).

Conclusion: 3D MR lumbosacral radiculography by Proset was useful for the detection of morphologic changes of the nerve root for the diagnosis of symptomatic foraminal stenosis.

Index terms
Foraminal Stenosis
Three-Dimension Magnetic Resonance Lumbosacral Radiculography
Proset

Received February 16, 2012; **Accepted** April 14, 2012
Corresponding author: Woo Mok Byun, MD
Department of Diagnostic Radiology, College of Medicine, Yeungnam University, 170 Hyeonchung-ro, Nam-gu, Daegu 705-717, Korea.
Tel. 82-53-620-3046 Fax. 82-53-653-5484
E-mail: wmbyun@med.yu.ac.kr

INTRODUCTION

Lumbar foraminal stenosis is a common pathologic entity of lumbar radioculopathy. The preoperative identification of the symptomatic lumbar foraminal stenosis is important because incidence of asymptomatic foraminal stenosis found by magnetic resonance (MR) imaging is quite high in asymptomatic elderly patients. The lack of recognition of this entity or inadequate treatment of nonspecific lateral canal stenosis is associated with failed back surgery syndrome (1-4).

MR imaging is widely used in the evaluation of lumbar foraminal stenosis. Morphologic changes of the foramen are well demonstrated on sagittal MR images (5). However, it is often difficult to differentiate between symptomatic and asymptomatic lumbar foraminal stenosis on conventional MR imaging.

In patients with lumbar foraminal stenosis, detection of morphologic changes of the nerve root rather than those of the foramen on MR imaging can reduce the incidence of failed back sur-

gery syndrome. There have been several reports on the nerve root morphology of symptomatic foraminal stenosis. Heithoff (6) stated that, on the basis of non-contrast CT scan data, affected nerve roots were enlarged, owing to edema distal to the impingement site in lateral stenosis. Aota et al. (7) reported that spinal nerve swelling and abnormality of the course of the nerve root in the foramen can be clearly depicted by magnetic resonance myelography (MRM). They further mentioned that MRM affords more specific information for the presurgical diagnosis of symptomatic foraminal stenosis compared with conventional MR imaging.

Lumbosacreal radiculography by the principles of the selective excitation technique (Proset) can provide excellent morphologic changes of the nerve root and dorsal root ganglion (DRG) (8).

The purpose of this study was to investigate the significance of three-dimension (3D) MR lumbosacral radiculography by Proset for the diagnosis of symptomatic foraminal stenosis.

MATERIALS AND METHODS

Subjects

The study was approved by the institutional review board of our hospital. All 71 patients who have lumbar foraminal stenosis on conventional MR imaging were selected from a database of MR examinations of the lumbar spine performed at our institution from October 2009 to November 2010. Among them, symptomatic patients whose leg or buttock pain was improved after selective decompression or whose clinical symptoms were provoked or improved after selective nerve root block for lumbar foraminal stenosis were included in the study. We excluded patients who had previous lumbar surgery, history of trauma, lumbar scoliosis, infection, tumor or fracture. Thus, of the 71 patients screened, 48 met the inclusion criteria for this study. The patient group consisted of 33 women and 15 men aged from 32 to 85 years (average, 69.5 years).

MR Imaging Protocol

MR imaging was performed with a 1.5-T scanner (Interna, Philips Medical System, Best, the Netherlands) with a spine array coil. On conventional spin-echo sequences, axial and sagittal T1- {583/12 [repetition time (TR) msec/echo time (TE) msec]} and turbo-T2-weighted images (3800/128) were performed in all cases. 3D coronal fast-field echo (FFE) sequences with selective water excitation using the Proset were acquired with the following acquisition parameters; 1 mm section thickness with a 1 mm overlapping section gap; 250 mm field of view; 256 × 256 matrix; TR, 23.2 ms; TE, 13.8 ms; 8° flip angle, and 2 signal intensity acquisitions. The angle of images was parallel to the longitudinal axis of the lumbar spinal cord and centered on the level of the L3 body. The perpendicular regional saturation slabs were used to suppress the signal intensity from the vessels. Forty original coronal FFE images for each subject (anteroposterior thickening of the resultant whole-imaging slab: 40 mm) were obtained. Imaging processing consists of direct volume rendering. For image processing, an Aquarius 3D workstation equipped with commercially available automated analysis 3D rendering software (TeraRecon Inc., San Mateo, CA, USA) was used.

Imaging Analysis

Conventional MR and 3D MR lumbosacral radiculography by Proset imaging, were retrospectively analyzed by two experienced neuroradiologists (reader 1 and 2) who had 20 and 7 years of experience, respectively. Images of the symptomatic and asymptomatic lumbar foraminal stenosis were randomly mixed for interpretation to avoid a bias. To assess reliability, both radiologists evaluated the MR images of the selected cases independently and were unaware of the clinical information and the outcome of surgery or selective nerve root block. Reader 1 evaluated the MR images and 3D MR lumbosacral radiculography by Proset imaging of the selected cases after 6 months.

A total of 288 foramina and corresponding nerve roots in 48 patients were analyzed from the L3-4 to the L5-S1 levels. Of these, 192 foramina of the L1-2 and the L2-3 levels were excluded because the lumbar foraminal stenosis in these levels is rare. Through conventional MR imaging without 3D MR lumbosacral radiculography, a total of 288 foramina were evaluated for identification of the presence of lumbar foraminal stenosis. If there was a discordant case, this interpretation was made in consensus. Moreover, each radiologist independently assessed morphologic changes of the corresponding nerve roots on the side and level of the lumbar foraminal stenosis on 3D MR lumbosacral radiculography. Morphologic changes included swelling, indentation, and tilting angle abnormality of the nerve roots.

Swelling of DRG and nerve roots was diagnosed when its size was bigger than that of the normal contralateral side of the same

level. The tilting angle of the nerve root was measured using a parallel line to the thecal sac and another line passing through the center of the preganglionic and postganglionic existing nerve roots and parallel to its long axis. Tilting angle of the nerve root was defined as abnormal if the nerve shifted upward with the angle offset more cephalad compared with the contralateral nerve root.

Statistical Analysis

The statistical analyses were performed using the Statistical Package for the Social Sciences (SPSS) for Windows (version 19.0; SPSS Inc., Chicago, IL, USA). Interobserver variability and intraobserver variability (reader 1) were analyzed by kappa statistics. A kappa value of less than 0.20 indicated slight; 0.21-0.40, fair; 0.41-0.60, moderate; 0.61-0.80, substantial; and 0.81 or greater, nearly perfect agreement (9). The χ^2 test was used to analyze ratios. A *p*-value less than 0.05 was deemed to be statistically significant.

RESULTS

Foraminal Stenosis on Conventional MR Imaging (Table 1)

Lumbar foraminal stenosis on conventional MR imaging was found in 63 of 288 foramina (23.1%) (from the L3-4 to L5-S1 levels) in 48 patients. Among them, a higher incidence of lumbar foraminal stenosis was found on the left side (43 foramina, 68.3%) than the right side (20 foramina, 31.7%). In the 63 foramina with lumbar foraminal stenosis, 49 (77.8%) were found to have symptomatic foraminal stenosis, while 14 (22.2%) were found to have asymptomatic foraminal stenosis. The most commonly involved level of lumbar foraminal stenosis in this study was the L5-S1 (54.0%), followed by L4-5 (42.8%), and L3-4 (3.2%). The incidence of lumbar foraminal stenosis in women (33 patients, 68.75%) was higher than in men (15 patients, 31.25%).

Evaluation of Three Morphologic Changes on 3D MR Lumbosacral Radiculography in Foraminal Stenosis

Swelling of the Nerve Root (Table 2)

Interobserver and intraobserver agreement of the recognition of swelling of the nerve root was nearly perfect (κ value: interobserver, 0.935; intraobserver, 1). The swelling of the nerve root was found in 36 of the 49 foramina with symptomatic foraminal stenosis (Fig. 1). Only one foramen of the asymptomatic foraminal stenosis showed swelling of the nerve root. The incidence of swelling of the nerve root in the L5-S1 level (22 foramina) was higher than in the L4-5 level (13 foramina). The swelling of the nerve root had a statistically valuable meaning

Table 1. Incidence of Lumbar Foraminal Stenosis on Conventional Magnetic Resonance Imaging

	L3-4	L4-5	L5-S1	Total
Asymptomatic foramina	0/94 (0/0)	7/76 (3/4)	7/69 (5/2)	14/239 (8/6)
Symptomatic foramina	2/2 (0/2)	20/20 (6/14)	27/27 (6/21)	49/49 (12/37)
Sensitivity (TP/TP + FN) (%)	100.0	100.0	100.0	100.0
Specificity (TN/TN + FP) (%)	100.0	90.8	89.9	94.1
Positive predictive value (%)	100.0	74.1	79.4	77.8
Negative predictive value (%)	100.0	100.0	100.0	100.0

Number of lumbar foraminal stenosis/total number of foramina. Number in parentheses indicates the number of the side of foramina with lumbar foraminal stenosis (right/left side).
Note.—FN = false negative, FP = false positive, TN = true negative, TP = true positive

Table 2. Incidence of Nerve Root Swelling in Lumbar Foraminal Stenosis on 3D Lumbosacral Radiculography

	L3	L4	L5	Total
Asymptomatic foraminal stenosis	0/0	0/7	1/7	1/14
Symptomatic foraminal stenosis	1/2	13/20	22/27	36/49
Sensitivity (TP/TP + FN) (%)	50.0	65.0	81.5	73.5
Specificity (TN/TN + FP) (%)	NA	100.0	85.7	92.9
Positive predictive value (%)	100.0	100.0	95.7	97.3
Negative predictive value (%)	0.0	50.0	54.5	50.0

Number of nerve roots with swelling/total number of nerve roots.
There was statistically significant difference in swelling of the nerve root among asymptomatic and symptomatic foraminal stenosis (χ^2 test, $p < 0.001$).
Note.—FN = false negative, FP = false positive, NA = not assessed, TN = true negative, TP = true positive, 3D = three-dimension

in symptomatic foraminal stenosis (χ^2 test, $p < 0.001$).

Indentation of Nerve Root (Table 3)

Interobserver and intraobserver agreement in recognition of the indentation of the nerve root was nearly perfect (κ value: interobserver, 0.925; intraobserver, 0.922). Of the 49 foramina with symptomatic foraminal stenosis, 18 were found to have indentation of the nerve root (Fig. 2). Of the 14 foramina with asymptomatic foraminal stenosis, only one showed indentation of the nerve root, which was statistically significant for symptomatic foraminal stenosis (χ^2 test, $p = 0.047$).

Tilting Angle Abnormality of Nerve Root (Table 4)

Interobserver agreement in recognition of the tilting angle abnormality of the nerve root was substantial (κ value: 0.78). Intraobserver agreement in recognition of the tilting angle abnormality of the nerve root was nearly perfect (κ value: 0.81). This abnormality was found in 10 of the 49 foramina with symptomatic foraminal stenosis (Fig. 3). There was no statistically significant meaning in symptomatic foraminal stenosis (χ^2 test, $p = 0.100$), however the tilting angle abnormality was not found in the asymptomatic foraminal stenosis.

Three Morphologic Changes of Nerve Root

One or more of the three morphologic findings of nerve root was found in 46 foramina (93.9%) of the symptomatic lumbar foraminal stenosis (Table 5). In 12 (85.7%) of 14 foramina with asymptomatic foraminal stenosis, any finding of morphologic changes was not found in this study (Fig. 4). The one or more of the three morphologic findings of the nerve root had a statisti-

Table 3. Incidence of Indentation of Nerve Root in Lumbar Foraminal Stenosis on 3D Lumbosacral Radiculography

	L3	L4	L5	Total
Asymptomatic foraminal stenosis	0/0	0/7	1/7	1/14
Symptomatic foraminal stenosis	0/2	7/20	11/27	18/49
Sensitivity (TP/TP + FN) (%)	0.0	35.0	40.7	36.7
Specificity (TN/TN + FP) (%)	NA	100.0	85.7	92.9
Positive predictive value (%)	NA	100.0	91.7	94.7
Negative predictive value (%)	0.0	35.0	27.3	29.54

Number of the nerve root with indentation/total number of nerve root.
There was statistically significant difference in indentation of the nerve root among asymptomatic and symptomatic foraminal stenosis (χ^2 test, $p = 0.047$).
Note.—FN = false negative, FP = false positive, NA = not assessed, TN = true negative, TP = true positive, 3D = three-dimension

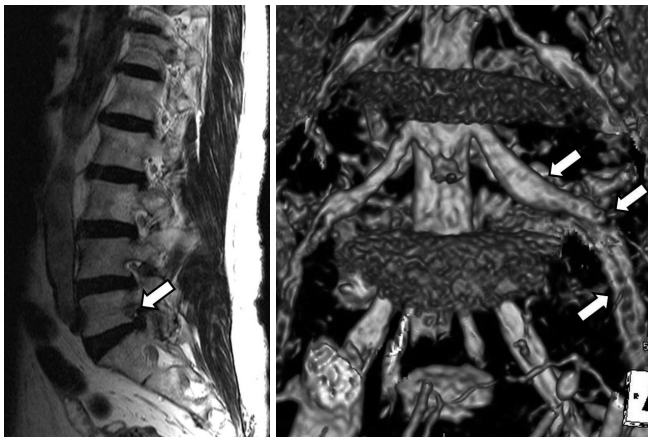

A B

Fig. 1. Sixty-five-year-old female with left leg pain.
A. Sagittal T2-weighted image shows a stenotic foramen (arrow) at L5-S1.
B. On 3D MR lumbosacral radiculography by Proset imaging, the swelling of the nerve root and dorsal root ganglion is demonstrated (arrows).
Note.—MR = magnetic resonance, Proset = principles of the selective excitation technique, 3D = three-dimension

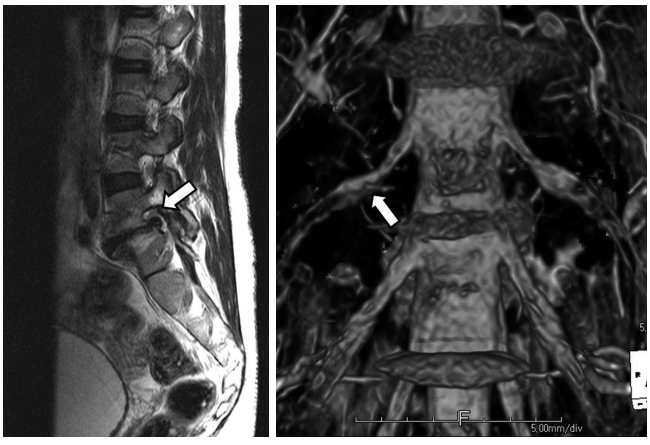

A B

Fig. 2. Thirty-two-year-old female with right leg pain.
A. Sagittal T2-weighted image shows a stenotic foramen (arrow) at L5-S1.
B. On 3D MR lumbosacral radiculography by Proset imaging, the indentation of the nerve root is demonstrated (arrow).
Note.—MR = magnetic resonance, Proset = principles of the selective excitation technique, 3D = three-dimension

cally valuable meaning in symptomatic foraminal stenosis (χ^2 test, $p < 0.001$).

A statistically significant difference was found among the three morphologic changes of the nerve root in symptomatic foraminal stenosis (χ^2 test, $p < 0.001$). In symptomatic foraminal stenosis, swelling was found in 36 foramina (73.5%), while indentation was found in 18 foramina (36.7%), and tilting angle abnormality was found in 10 foramina (20.4%).

Table 4. Incidence of the Tilting Angle Abnormality of Nerve Root in Lumbar Foraminal Stenosis on 3D Lumbosacral Radiculography

	L3	L4	L5	Total
Asymptomatic foraminal stenosis	0/0	0/7	0/7	0/14
Symptomatic foraminal stenosis	1/2	2/20	10/27	10/49
Sensitivity (TP/TP + FN) (%)	50.0	10.0	37.0	20.4
Specificity (TN/TN + FP) (%)	NA	100.0	100.0	100.0
Positive predictive value (%)	100.0	100.0	100.0	100.0
Negative predictive value (%)	0.0	28.0	29.2	26.4

Number of nerve roots with tilting angle abnormality/total number of nerve roots.
There was no statistically significant difference in the tilting angle abnormality of the nerve root among asymptomatic and symptomatic foraminal stenosis (χ^2 test, $p = 0.100$).
Note.—FN = false negative, FP = false positive, NA = not assessed, TN = true negative, TP = true positive, 3D = three-dimension

Table 5. Incidence of Three Morphologic Changes of Nerve Root in Lumbar Foraminal Stenosis on 3D Lumbosacral Radiculography

	L3	L4	L5	Total
Asymptomatic foraminal stenosis	0/0	0/7	2/7	2/14
Symptomatic foraminal stenosis	1/2	19/20	26/27	46/49
Sensitivity (TP/TP + FN) (%)	50.0	95.0	96.3	93.9
Specificity (TN/TN + FP) (%)	NA	100.0	71.4	85.7
Positive predictive value (%)	100.0	100.0	92.6	95.8
Negative predictive value (%)	0.0	87.5	83.3	80.0

Number of nerve roots with one or more of the three morphologic changes/total number of nerve roots.
There was statistically significant difference in three morphologic findings of the nerve root among asymptomatic and symptomatic foraminal stenosis (χ^2 test, $p < 0.001$).
Note.—FN = false negative, FP = false positive, NA = not assessed, TN = true negative, TP = true positive, 3D = three-dimension

A B

Fig. 3. Seventy-nine-year-old female with left leg pain.
A. Sagittal T2-weighted image shows a stenotic foramen (arrow) at L5-S1.
B. On a 3D MR lumbosacral radiculography by Proset imaging, the swelling and tilting angle abnormality of the nerve root are demonstrated (arrows).
Note.—MR = magnetic resonance, Proset = principles of the selective excitation technique, 3D = three-dimension

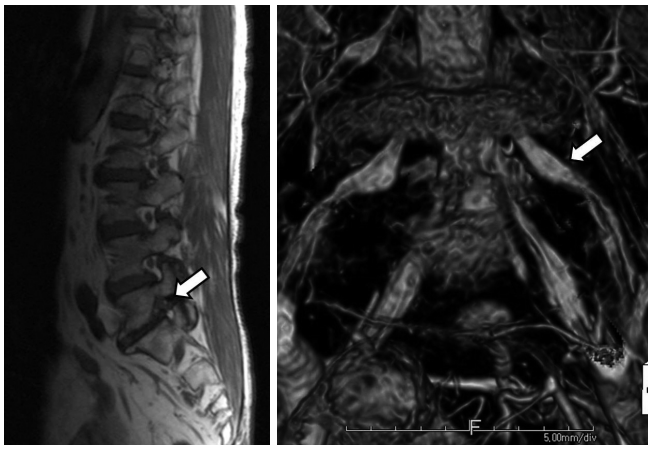

A B

Fig. 4. Seventy-three-year-old female with back pain without radiculopathy.
A. Sagittal T2-weighted image shows a stenotic foramen (arrow) at L5-S1.
B. On 3D MR lumbosacral radiculography by Proset imaging, the morphologic change of the nerve root is not demonstrated (arrow).
Note.—MR = magnetic resonance, Proset = principles of the selective excitation technique, 3D = three-dimension

DISCUSSION

Lumbar foraminal stenosis is defined as the narrowing of the bony exit of the nerve root caused by a decrease in the height of an intervertebral disc, osteoarthritic changes in the facet joints, cephalad subluxation of the superior articular process of the inferior vertebra, and buckling of the ligamentum flavum or protrusion of the annulus fibrosus (10). Lumbar foraminal stenosis may result in lumbar radiculopathy. However, the incidence of asymptomatic foraminal stenosis is quite high in asymptomatic elderly patients (4). For appropriate treatment or reducing failed back surgery syndrome, identification of symptomatic lumbar foraminal stenosis is important. Symptomatic nerve roots caused by foraminal stenosis can reliably be identified by selective nerve root blocks (11). However, the procedure is invasive and painful for patients and it may cause mechanical damage to a nerve root.

There have been several radiologic reports about lumbar foraminal stenosis. Wildermuth et al. (12), Kunogi and Hasue (4) and Lee et al. (13) reported about the grading or classification of lumbar foraminal stenosis. However, they did not mention the relationship between the degree of morphologic foraminal stenosis and clinical symptoms. Aota et al. (7) reported that spinal nerve swelling and abnormality over the course of the nerve root in the foramen could be clearly depicted by MRM. They further mentioned that spinal nerve swelling was significantly associated with symptomatic dorsal root ganglion compression. The sensitivity and specificity of spinal nerve root swelling were 60% and 96%, respectively, while normal volunteers had no spinal nerve root swelling. The sensitivity and specificity of the abnormal nerve root course were 96% and 83%, respectively, but this abnormality was also found in 13% of asymptomatic normal volunteers. The findings suggest that MRM adds additional and more specific information for the evaluation of symptomatic foraminal stenosis than conventional MR imaging. In the report, the sample size of 25 for symptomatic foraminal stenosis is small to make broad generalizations about the findings.

Proset imaging is a selective excitation technique used to suppress either water or fat by exploiting the difference between water and fat resonance frequencies. The signal intensity of fat was completely suppressed and the details of the DRGs were better delineated. The use of Proset imaging also does not increase scanning time. This technique is noninvasive and has no contrast adverse reaction. Previous reports on the evaluation of morphologic features and variations of normal human lumbar DRGs by Proset imaging has shown that the normal anatomy and variants of lumbar DRGs could be clearly demonstrated by 3D FFE MR imaging along with the water selective excitation technique (8). To the best of our knowledge, this technique has not been reported in the investigation of the significance of the diagnosis in symptomatic foraminal stenosis.

According to previous reports (3, 10), a higher incidence of lumbar foraminal stenosis is found in the left side and lower lumbar segments. The most common roots involved were the fifth lumbar root, followed by the fourth, third, and second, which was similar to the results of our study. This is explained by the size and location of the DRGs. The relatively larger and more proximally located DRGs in the lower lumbar region may be more susceptible to compression than the upper DRGs (8, 14).

In our study, three morphologic findings (the swelling, indentation, and tilting angle abnormality) of nerve roots in the foramina with lumbar foraminal stenosis were evaluated on source images of Proset imaging and 3D MR lymbosacral radiculography. The most frequent morphologic finding in symptomatic foraminal stenosis was the swelling of the nerve root, followed by the indentation and tilting angle abnormality. There was a statistically significant difference among the three morphologic changes of the nerve roots in symptomatic foraminal stenosis (χ^2 test, $p < 0.001$).

The association of spinal nerve swelling and DRG compression may be attributed to the histologic properties of DRGs. The nerve root compression causes changes of endoneurial capillary pressure. Increased capillary vascular permeability causes the breakdown of the blood-nerve barrier. A leakage of fluid and macromolecules from these vessels out into the endoneurial space result in intraneural edema formation (15). Rydevik et al. (16) applied acute compression to rat DRGs and found an almost threefold increase in endoneural fluid pressure. They also suggested that this elevation in DRG pressure could be the mechanism underlying the production of nerve root pain. On the other hand, in chronic cauda equina or nerve root compression, edema is not a prominent feature of nerve roots (15). No report to date has described changes in the spinal nerve in chronic DRG compression models.

The ubiquity of the results of the present study are limited in

that the negative predictive values (NPV) of the tests of three morphologic changes are lower than other test outcomes. A possible cause of the lower NPV is the smaller sample size (n = 14) for asymptomatic foraminal stenosis compared to the symptomatic foraminal stenosis (n = 49). Nevertheless, abnormal morphologic changes were found in only 2 of the foramina with asymptomatic foraminal stenosis.

In conclusion, with Proset imaging, the signal intensity of fat was completely suppressed and the details of the DRGs were better delineated. We found that three morphologic changes (the swelling, indentation, and tilting angle abnormality) of the nerve root by 3D MR lumbosacral radiculography by Proset imaging were statistically significant for the diagnosis of symptomatic foraminal stenosis. Nerve root swelling was more frequently found relative to the other two findings in symptomatic foraminal stenosis. We believe that 3D MR lumbosacral radiculography by Proset imaging was very useful for the detection of the morphologic changes of the nerve root in the diagnosis of symptomatic foraminal stenosis.

REFERENCES

1. Burton CV, Kirkaldy-Willis WH, Yong-Hing K, Heithoff KB. Causes of failure of surgery on the lumbar spine. *Clin Orthop Relat Res* 1981:191-199
2. Cramer GD, Cantu JA, Dorsett RD, Greenstein JS, McGregor M, Howe JE, et al. Dimensions of the lumbar intervertebral foramina as determined from the sagittal plane magnetic resonance imaging scans of 95 normal subjects. *J Manipulative Physiol Ther* 2003;26:160-170
3. Jenis LG, An HS. Spine update. Lumbar foraminal stenosis. *Spine (Phila Pa 1976)* 2000;25:389-394
4. Kunogi J, Hasue M. Diagnosis and operative treatment of intraforaminal and extraforaminal nerve root compression. *Spine (Phila Pa 1976)* 1991;16:1312-1320
5. Grenier N, Kressel HY, Schiebler ML, Grossman RI, Dalinka MK. Normal and degenerative posterior spinal structures: MR imaging. *Radiology* 1987;165:517-525
6. Heithoff KB. Computed tomography and plain film diagnosis of the lumbar spine. In Weinstein JN, Wiesel SW. *The Lumbar Spine*. Philadelphia: Saunders, 1990:283-319
7. Aota Y, Niwa T, Yoshikawa K, Fujiwara A, Asada T, Saito T. Magnetic resonance imaging and magnetic resonance myelography in the presurgical diagnosis of lumbar foraminal stenosis. *Spine (Phila Pa 1976)* 2007;32:896-903
8. Shen J, Wang HY, Chen JY, Liang BL. Morphologic analysis of normal human lumbar dorsal root ganglion by 3D MR imaging. *AJNR Am J Neuroradiol* 2006;27:2098-2103
9. Landis JR, Koch GG. The measurement of observer agreement for categorical data. *Biometrics* 1977;33:159-174
10. Hasegawa T, An HS, Haughton VM, Nowicki BH. Lumbar foraminal stenosis: critical heights of the intervertebral discs and foramina. A cryomicrotome study in cadavera. *J Bone Joint Surg Am* 1995;77:32-38
11. Herron LD. Selective nerve root block in patient selection for lumbar surgery: surgical results. *J Spinal Disord* 1989;2:75-79
12. Wildermuth S, Zanetti M, Duewell S, Schmid MR, Romanowski B, Benini A, et al. Lumbar spine: quantitative and qualitative assessment of positional (upright flexion and extension) MR imaging and myelography. *Radiology* 1998;207:391-398
13. Lee S, Lee JW, Yeom JS, Kim KJ, Kim HJ, Chung SK, et al. A practical MRI grading system for lumbar foraminal stenosis. *AJR Am J Roentgenol* 2010;194:1095-1098
14. Hasue M, Kunogi J, Konno S, Kikuchi S. Classification by position of dorsal root ganglia in the lumbosacral region. *Spine (Phila Pa 1976)* 1989;14:1261-1264
15. Olmarker K, Rydevik B, Holm S. Edema formation in spinal nerve roots induced by experimental, graded compression. An experimental study on the pig cauda equina with special reference to differences in effects between rapid and slow onset of compression. *Spine (Phila Pa 1976)* 1989;14:569-573
16. Rydevik BL, Myers RR, Powell HC. Pressure increase in the dorsal root ganglion following mechanical compression. Closed compartment syndrome in nerve roots. *Spine (Phila Pa 1976)* 1989;14:574-576

증후성 추공 협착증의 진단에서 Principles of the Selective Excitation Technique 영상기법을 이용한 삼차원 자기공명 요추천골 신경근조영술의 유용성

임지경 · 변우목

목적: 증후성 추공 협착증 진단에서 principles of the selective excitation technique (이하 Proset) 영상기법을 이용한 삼차원 자기공명 요추천골 신경근조영술의 유용성을 알아보고자 하였다.

대상과 방법: 고식적 자기공명영상에서 추공 협착증이 있는 48명의 환자를 대상으로 양측 L3-4부터 L5-S1까지 총 288개의 추공을 조사하였다. 고식적 자기공명영상을 통하여 추공 협착증의 여부를 조사하고, Proset 영상기법을 이용한 삼차원 자기공명 신경근조영술을 이용하여 해당 신경근의 세 가지 형태학적 변화(부종, 압흔 그리고 비정상적인 경사각도)를 평가하였다. 신경근의 형태학적 변화와 임상증상을 비교하였다.

결과: 48명의 환자에서 총 63개의 추공에서 추공 협착증이 발견되었고 이 중 49개는 증후성, 14개는 비증후성 추공 협착증으로 진단되었다. 증후성 추공 협착증에서 신경근의 부종, 압흔, 비정상적인 경사각도는 각각 36예, 18예 그리고 10예에서 관찰되었으며, 46개의 추공에서 3가지 형태학적 변화 중 1가지 이상의 변화가 관찰되었다. 비증후성 추공 협착증 중 12개의 추공에서는 신경근의 어떠한 형태학적 변화도 보이지 않았다. 증후성 추공 협착증에서 세 가지 형태학적 변화들은 통계학적으로 유의한 차이를 보였다(χ^2 test, $p < 0.001$).

결론: Proset 영상기법을 이용한 삼차원 자기공명 요추천골 신경근조영술은 신경근의 형태학적 변화를 볼 때 도움을 주고, 증후성 추공 협착증의 진단에 매우 유용한 기법이다.

영남대학교 의과대학 영상의학과학교실